Published in "Physical Review 79(5): 051403, 2009"
which should be cited to refer to this work.

Crystal structure of highly concentrated, ionic microgel suspensions studied by neutron scattering

U. Gasser*
Laboratory for Neutron Scattering, ETH Zurich & Paul Scherrer Institut, 5232 Villigen PSI, Switzerland and Adolphe Merkle Institut, University of Fribourg, Route de l'ancienne Papeterie, P.O. Box 209, 1723 Marly 1, Switzerland

B. Sierra-Martin and A. Fernandez-Nieves†
School of Physics, Georgia Institute of Technology, Atlanta, Georgia 30332-0430, USA

We present a neutron-scattering investigation of the crystal structure formed by *p*H-sensitive poly(2-vinylpyridine) microgel particles with 5 wt % of cross-linker. We focus on highly swollen particles and explore concentrations ranging from below close packing to well above close packing, where the particles are forced to shrink and/or interpenetrate. The crystal structure is found to be random hexagonal close packed, similar to the structure typically found in hard-sphere systems.

I. INTRODUCTION

Microgel particles are cross-linked polymer particles with sizes in the colloidal range that are suspended in a fluid. Many research activities are focused on microgels due to their potential in applications, which include responsive valves in microfluidic devices [1], drug delivery [2], and novel optical switches [3]; this results from the responsiveness of microgels to changes in their environment [4], including variations in temperature, solvent *p*H, or salt concentration.

It is this responsiveness of microgel particles which makes them also interesting as model systems for investigations of fundamental thermodynamic questions; the particle diameter and the interaction potential can be varied by changing an experimentally accessible parameter such as the *p*H of the solvent. This makes microgels ideal systems for studying the phase behavior and the phase transitions of particles with interactions ranging from hard-sphere-like to very soft potentials. While considerable progress has been made in the understanding of the phase behavior of hard and soft spheres [5], there are still many open questions concerning the glass transition at high densities [6], the process of crystal nucleation and growth [7], and the phase behavior that should be expected for very soft particles [8]. In suspensions of microgels many aspects of these questions can be studied in one and the same experimental system allowing flexible control of both volume fraction and the pair potential.

In this paper we focus on the crystal structure that is obtained in soft charged microgels at very high densities. While the maximum volume fraction, ϕ, of hard spheres is limited by close packing with fcc or hcp structure to values ≤ 0.74, the particle density of microgels can be increased further, such that the particles are forced to shrink and/or interpenetrate. So far, only one experiment has been reported on the crystal structures observed in ionic microgels at high densities [9]; crystals with fcc structure and a coexistence of fcc and bcc were observed in a system of particles consisting of poly-N-isopropyl acrylamide (PNIPAM) copolymerized with acrylic acid. In neutral microgels Hellweg *et al.* [10] also found crystals with fcc structure, suggesting that there is no fundamental difference between the structure of hard-sphere-like colloids and that of softer microgel particles. Furthermore, a rheology study gave evidence that suspensions of PNIPAM particles with screened charge repulsion behave like hard spheres in the swollen state [11]. Both the formation of crystals and the rheological behavior close to the glass transition at effective volume fractions in the range from 0.4 to 0.63 were found to be in good agreement with hard spheres. By contrast, recent theoretical calculations suggest a much more complex phase behavior for suspensions of very soft charged particles [8]. At very high concentrations a behavior fundamentally different from that of hard-sphere particles is expected; noncubic crystal structures such as hexagonal or trigonal lattices are expected to form. Additionally, for systems with strong steric repulsions, such as micelles or highly cross-linked microgels, the structure minimizing the free energy of the system is, at high enough densities, the so-called $A15$, which is a bcc lattice with eight basis atoms in the unit cell [12].

II. EXPERIMENTAL METHODS

A. Experimental system

We used particles consisting of poly(2-vinylpyridine) (2VP) cross-linked with divinylbenzene (DVB) (5 wt %). 2,2′-azobis(2-amidinopropane) dihydrochloride was used as initiator for the polymerization reaction. The synthesis is described in Ref. [13]. Based on the higher reaction rate of the cross-linker with respect to the monomer, we expect our particles to have an inhomogeneous distribution of DVB. This is also the case for other microgels, as shown by polymerization kinetic studies [14,15], and with light [16] and neutron [17–20] scattering.

In water, the particles swell for $p\mathrm{H} \lesssim 4$ due to the ionization of the 2VP groups, as shown in Fig. 1, where we plot the particle size measured by dynamic light scattering as a func-

*urs.gasser@psi.ch
†alberto.fernandez@physics.gatech.edu

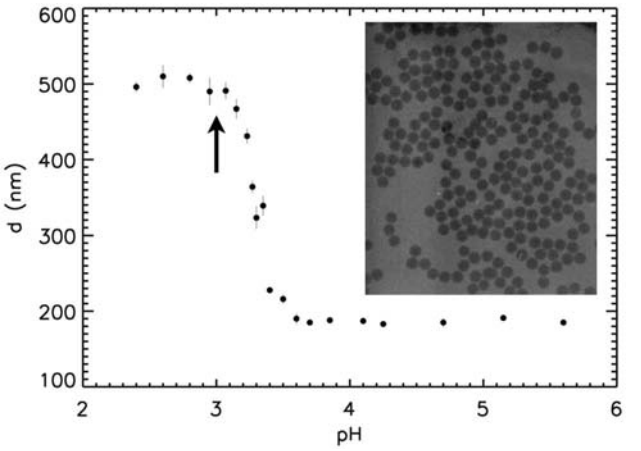

FIG. 1. Hydrodynamic diameter of 2VP particles measured by dynamic light scattering as a function of solvent pH. The arrow indicates the pH and diameter of the particles used in this study. A TEM image of particles in the shrunken state is shown in the inset. The good monodispersity of the particles is apparent.

tion of the solution pH. In addition, the particles carry a surface charge due to the initiator employed in the synthesis; this charge is located at the periphery of the particles [21] and stabilizes the particles by electrostatic repulsion, particularly in their deswollen state, for $p\mathrm{H} \gtrsim 4$. The suspension is monodisperse, as illustrated by the transmission electron microscopy (TEM) image of Fig. 1. From this image, we determine a size of $d_{\mathrm{TEM}}=(182\pm5)$ nm, which we take as a reasonable estimate of the collapsed size of the microgel particles.

We worked at $p\mathrm{D}=3$, where the particles are completely swollen. "pD" is used instead of "pH" since the solvent and the acid are deuterated. Since the synthesis was performed in water, we freeze-dried the sample, redispersed the particles in heavy water (D_2O) and increased the concentration using a rotary evaporator. By adding DCl, we changed the pD to three thus obtaining an initial sample at a very high concentration, where the particles are forced to shrink due to the limited volume of the sample. Lower particle concentrations were obtained by dilution with D_2O, always adjusting the pD to three with DCl.

A small amount of the more concentrated sample was dried completely in order to obtain a measure of the weight concentration, which we relate to the particle number concentration, c, using the size measured by TEM. Since the volume fraction ϕ is not a good measure of concentration in the case of microgels, as these particles can shrink at high enough densities, we use $\xi=cV_0^{c=0}$, with $V_0^{c=0}$ the volume of a single particle in the swollen state in a sample with a low particle density, $c\approx0$. Concentrated samples with $\xi\geq0.70$ were found to fully crystallize within hours after manually shaking the samples, which could be verified visually since the Bragg reflection corresponding to the largest lattice spacing could be observed with visible light. The higher value of ξ compared to that for hard-sphere crystallization is consistent with particles interacting with soft potentials, as shown by Senff and Richtering [22] with neutral microgel particles. All measurements were performed after leaving the samples for at least 24 h in the experimental cells.

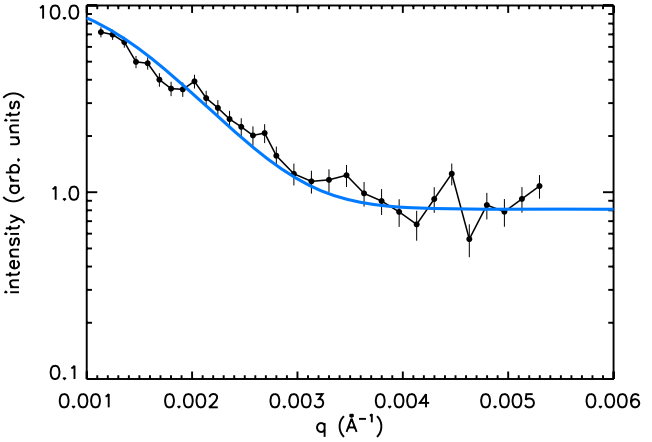

FIG. 2. (Color online) Form factor determined by USANS at $\xi=0.15$ (connected black dots) compared with the smoothed form factor obtained from SANS (line; see Fig. 3). The fit takes the q smearing of the USANS instrument into account.

B. Ultrasmall-angle neutron-scattering

Data for four crystalline samples and a dilute sample were taken on the Bonse-Hart type BT5 ultrasmall-angle neutron-scattering (USANS) instrument at the National Institute of Standards and Technology (NIST) (Gaithersburg, MD) [23]. USANS is the method of choice for measuring structures with a typical size >400 nm with neutrons. The resolution of the BT5 instrument is excellent in the scattering plane ($\Delta q_x=2.6\times10^{-5}$ Å^{-1}) but the slit geometry of the perfect Si single-crystal monochromator and analyzer causes a smearing of the scattered intensity in the perpendicular direction over a large q_y range. Since this smearing is well known, it can be taken into account when the data is fitted with a model. Therefore, quite detailed information about the crystal structure can be obtained from both the positions and the widths of the observed peaks in the range $10^{-4}<q<6\times10^{-3}$ Å^{-1}, which is the region of interest for our microgel suspensions.

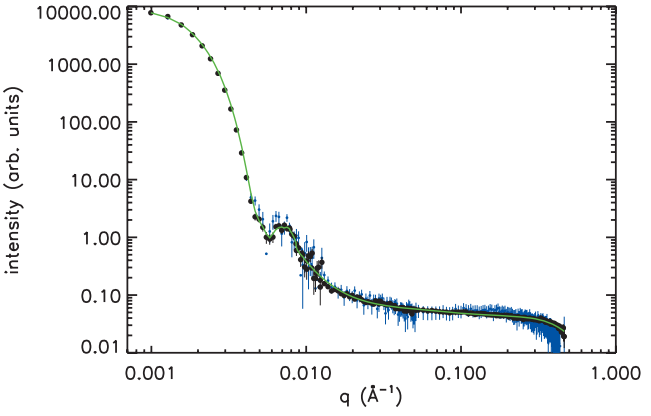

FIG. 3. (Color) Form factor measured with SANS in a sample with $\xi=0.03$ (blue) and $\xi=0.15$ (black). A smoothed fit to the data is shown by the green line. The backgrounds due to D_2O and dark counts are subtracted from the data shown. For $q<0.004$ Å^{-1}, the measurements at both ξ agree very well and, therefore, the blue data points are hidden by the black ones.

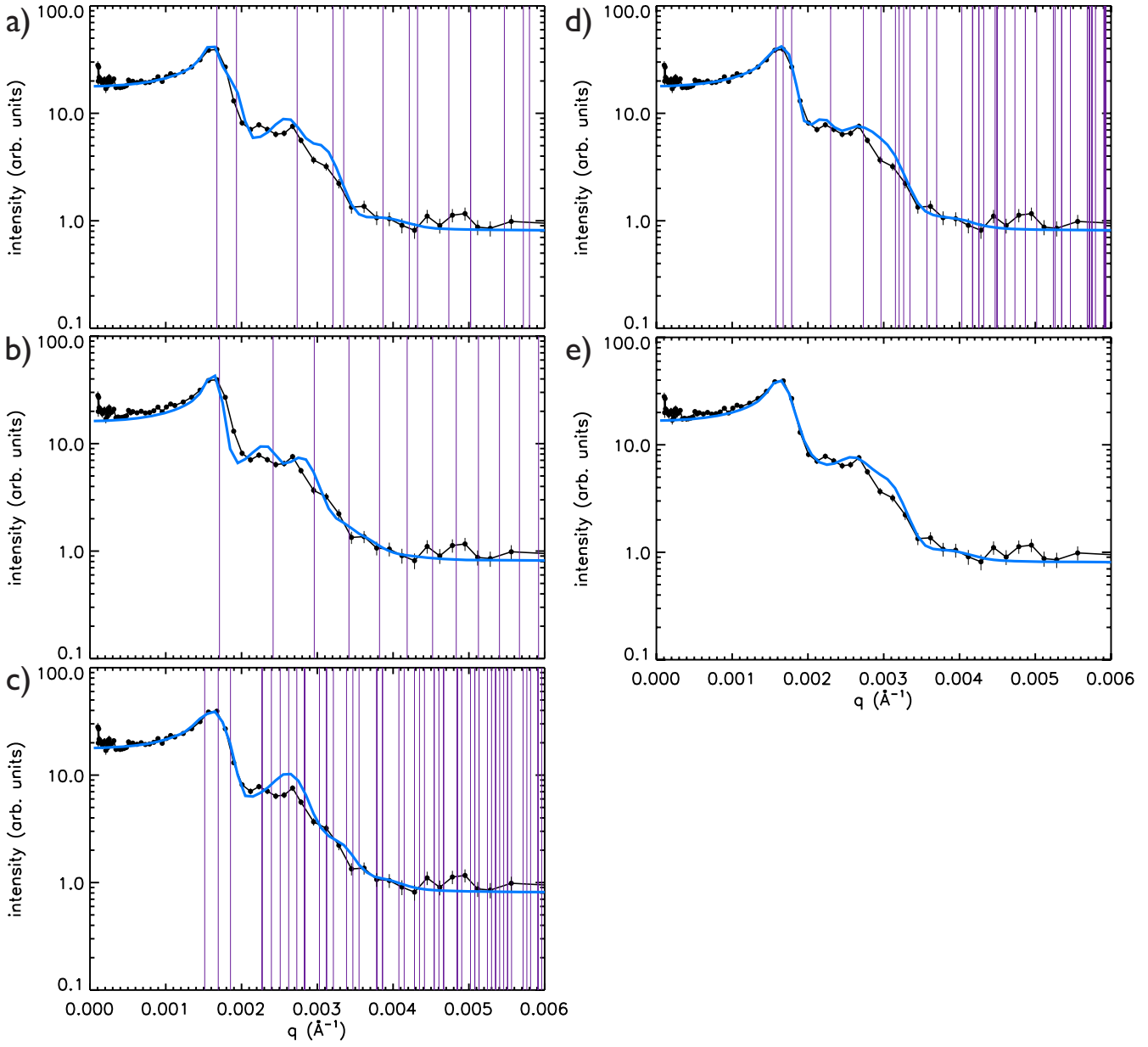

FIG. 4. (Color online) USANS measurement at ξ=0.80 compared with fits for various structures: (a) fcc, (b) bcc, (c) *A*15, (d) hcp, and (e) rhcp. The positions of the Bragg peaks are shown by the vertical lines except for rhcp, which we take as a random mixture of fcc and hcp with a slight tendency toward hcp.

The differential scattering cross section, $d\Sigma/d\Omega(q)$, has to be smeared along the q_y direction corresponding to the slits of the Si crystals to obtain the smeared cross section, $d\Sigma/d\Omega_s(q)$, which is measured by USANS:

$$\frac{d\Sigma}{d\Omega_s}(q) = \frac{1}{\Delta q_y}\int_0^{\Delta q_y} \frac{d\Sigma}{d\Omega}(\sqrt{q^2+u^2})du, \qquad (1)$$

where Δq_y=0.117 Å^{-1} is a fixed parameter of the instrument [23]. Furthermore, the wavelength spread $\Delta\lambda/\lambda$=0.06 (λ=2.38 Å) of the neutrons reaching the sample causes another smearing of the measured data, which is, however, much smaller than the one given by Eq. (1).

C. Small-angle neutron-scattering

Small-angle neutron-scattering (SANS) measurements were performed using the SANS-I instrument at SINQ (PSI, Villigen, Switzerland) and the NG3 SANS instrument at NIST (Gaithersburg, MD). While the resolution of a SANS instrument is not expected to be sufficient for resolving in detail structures with a size of ~500 nm, SANS is a powerful method for determining the form factor of the used particles in samples with low concentration. The measurements on the NG3 SANS instrument were done with a neutron wavelength λ=8.4 Å and a larger wavelength of λ=12 Å was used on SANS-I to improve the q resolution, which is determined by the wavelength resolution, $\Delta\lambda$, and by the resolution of the scattering angle, θ:

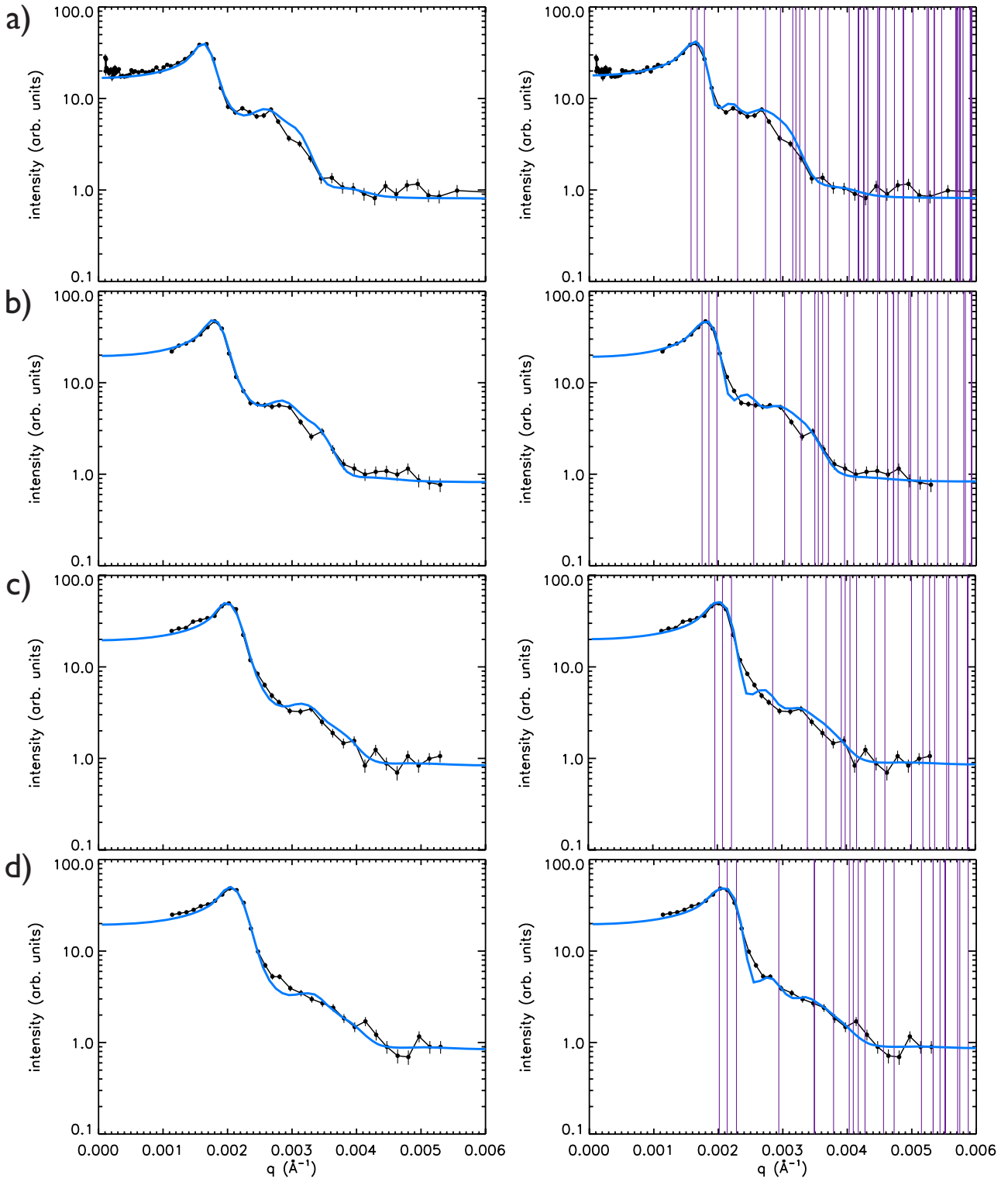

FIG. 5. (Color online) USANS measurements at (a) ξ=0.80, (b) 1.10, (c) 1.50, and (d) 1.75 compared with fits for rhcp (left) and hcp (right) structures.

$$\frac{\Delta q}{q} = \frac{\Delta \lambda}{\lambda} + \frac{\Delta \theta}{\theta}. \qquad (2)$$

In our experiments, $\Delta\lambda/\lambda$ is given by the wavelength resolution of the neutron velocity selector used to obtain a quasi-monochromatic beam and was fixed to 0.1 on both SANS instruments. $\Delta\theta/\theta$ was reduced by choosing long collimation and sample to detector distances of 13.2 m on NG3 SANS and 18 m on SANS-I, and by focusing the neutron beam on the detector with neutron lenses [24] on both instruments.

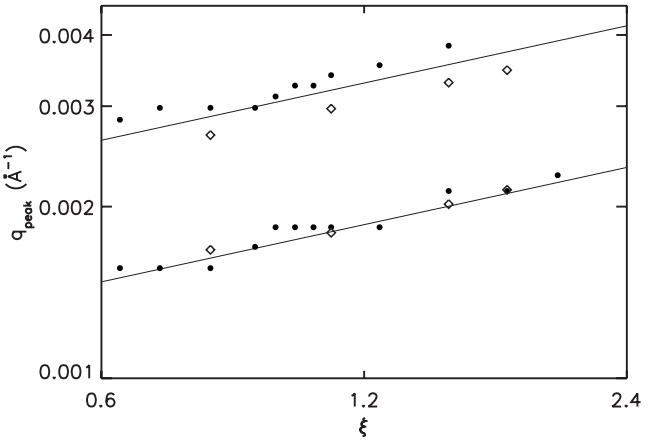

FIG. 6. Peak positions obtained by SANS (●) and USANS (◇) as a function of the concentration ξ. The behavior expected for a simple compression of the structure with increasing ξ is shown by the lines, $q_{\text{peak}} \sim \xi^{1/3}$.

The q resolution given by Eq. (2) is taken into account in fits to the SANS measurements.

III. RESULTS AND DISCUSSION

A. Form factor

The form factor $F(q)$ of the microgel particles was measured by USANS for a suspension at $\xi=0.15$, as shown in Fig. 2. The noise in this data results from the low scattering contrast of the microgels, which are highly swollen at pD $=3$ and from the low beam intensity of the USANS line, which would have required massive counting times in order to improve the measurement statistics. We also emphasize that despite the relatively high particle concentration, the interactions between particles remain rather insignificant; this results from the charge neutralization exerted by the counterions inside each particle. At pD$=3$, these microgels are fully ionized and attract counterions, which rise the osmotic pressure inside the microgels causing their swelling. Under these conditions, the particles are essentially neutral and thus no significant interaction is expected between them at this relatively low volume fraction.

To measure $F(q)$ more accurately, we also performed SANS measurements at $\xi=0.03$ and 0.15 that are shown in Fig. 3, where backgrounds due to D_2O and dark counts are subtracted. As there is no significant difference between these two measurements, we conclude that the $\xi=0.15$ data can be used as an accurate measurement of the form factor. We performed a smoothing of the $\xi=0.15$ data and used this as an approximation for the particle form factor for all SANS measurements.

We further compared the USANS result with that obtained by SANS after properly smearing the differential scattering cross section, $d\Sigma/d\Omega(q)$, obtained by SANS according to Eq. (1). The result is shown in Fig. 2 and agrees very well with the USANS measurement. We will thus use this smoothed $F(q)$ to obtain the structural information from the USANS measurements at higher particle concentrations.

B. Crystal structure

Using the previously determined form factor and the known particle concentration, we normalize our data to obtain the structure factor, $S(q)$. The results are shown in Fig. 4 for $\xi=0.80$ and in Fig. 5 for all the studied values of ξ. Some structural features are clearly observable. To understand these observations, we calculate $S(q)$ for fcc, bcc, $A15$, hcp, and random hexagonal close packing (rhcp). rhcp [25,26], a random mixture of fcc and hcp, is expected for particles that are similar to hard spheres, and bcc is found for particles with charge repulsion at relatively low volume fractions and solvents with low salt concentration. The $A15$ structure has been observed in dendritic polymers [27] and it is predicted for systems with strong steric repulsions between the particles, as it minimizes the contact area between neighboring particles [12,28]. The structure factor is modeled as the sum of all Bragg peaks of a polycrystalline sample: $S(q) = \Sigma_{i,j,k} p(q - Q_{i,j,k})$, where $\boldsymbol{Q}_{i,j,k} = i\boldsymbol{b}_x + j\boldsymbol{b}_y + k\boldsymbol{b}_z$ is a lattice position in reciprocal space; $\mathbf{b}_\alpha$ are the corresponding lattice vectors. The Bragg peaks are approximated by Gaussians, $p(q)$, with a width given by the q resolution corresponding to the wavelength spread of the BT5 instrument. We fit the experimental results of Fig. 4 leaving the nearest-neighbor distance as free parameter, which is expected to decrease for high ξ. The comparison of the fits and the experiment are also shown in Fig. 4, where the expected positions of the Bragg peaks are shown as well. Since we use a form factor measured with a dilute sample at these high concentrations, $F(q)$ is merely an approximation. However, the Bragg peaks we are mainly interested in lie in the range $0.001 < q < 0.004$ Å^{-1}, where the form factor decays monotonously. Therefore, we expect only discrepancies in height between the measured intensity curves and the fits. Consequently, such differences should not be overrated, and we have concentrated on fits that reproduce the peak positions and peak widths as well as possible. As shown in Fig. 5, however, even at very high concentrations we do not observe large intensity discrepancies between the fits and the measurements, which confirms that the form factor used is not too crude an approximation.

Some structures can clearly be ruled out since they do not reproduce the positions or the widths of the observed peaks. For fcc a shoulder in the first peak would be expected due to a Bragg peak at $q \approx 0.0019$ Å^{-1}, as shown in Fig. 4(a). Furthermore, the small peak observed at $q=0.0022$ Å^{-1} is not compatible with fcc and we conclude that pure fcc does not agree with the measurement. In the case of bcc the first peak would be expected to be narrower, as shown in Fig. 4(b). The first peak at $q \approx 0.0016$ Å^{-1} can be reproduced well with $A15$. However, in contrast to the measurement a clear broad peak at $q \approx 0.0026$ Å^{-1} would be expected, as shown in Fig. 4(c). hcp and rhcp give the best fits to the measured data, as shown in Figs. 4(d) and 4(e). We have also considered the $cI16$ structure, which is a bcc structure with a basis of eight particles, and is known from high-pressure structures of silicon and lithium [29,30]. It might be expected for particles with a relatively soft repulsion at a distance close to the diameter of a particle and a stronger repulsion at a somewhat smaller distance that is relevant at high concentrations. How-

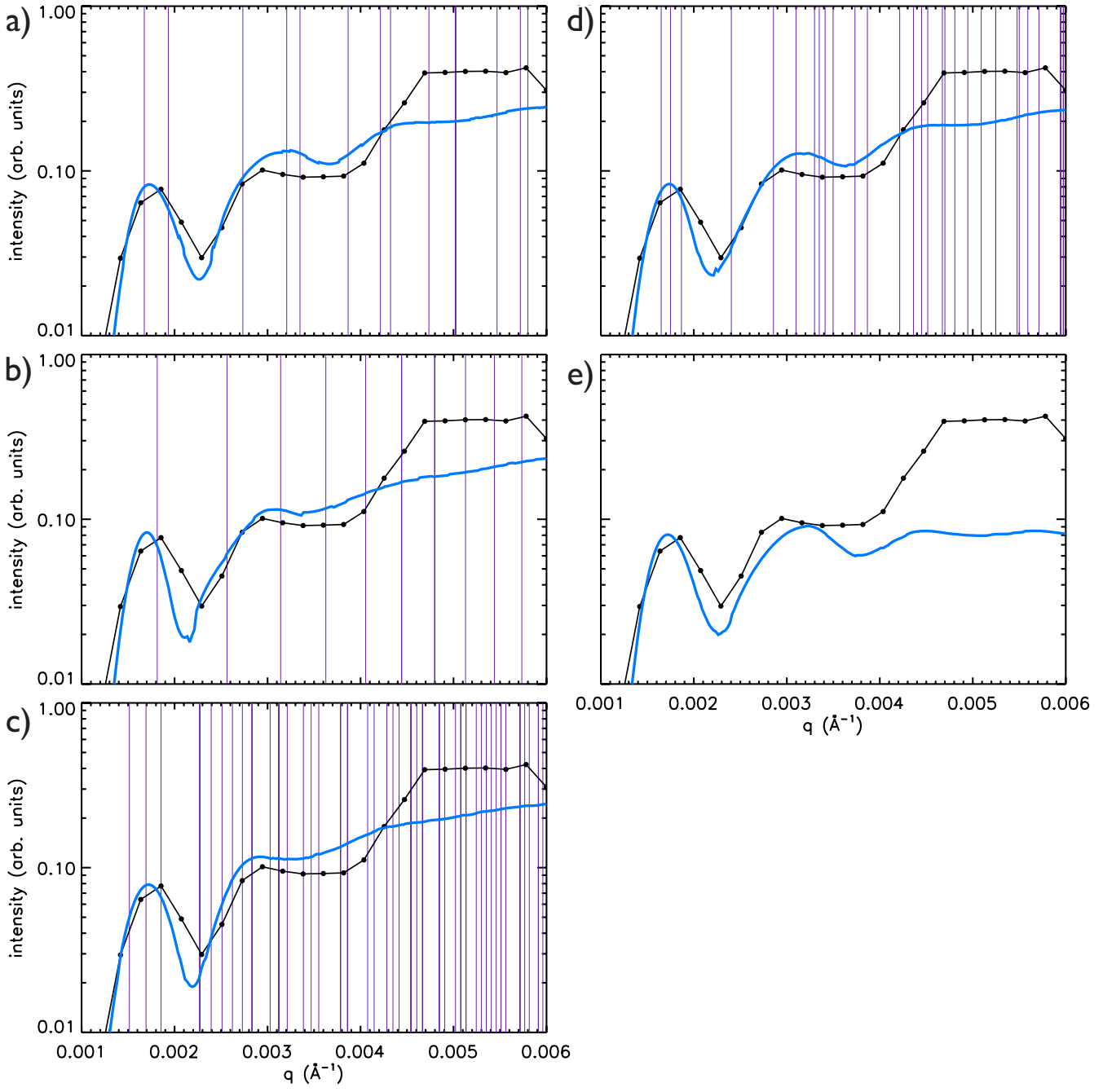

FIG. 7. (Color online) SANS measurement (ξ=0.80) divided by the form factor shown in Fig. 3 (black dots). The measurement is compared with fits for (a) fcc, (b) bcc, (c) $A15$, (d) hcp, and (e) rhcp structures (blue lines). The positions of the expected Bragg peaks are shown by the vertical lines for all structures except for rhcp. The fits take the limited q resolution of the SANS instrument into account.

ever, we find that, similar to $A15$, $cI16$ clearly does not agree with the measured structure.

As ξ is increased from 0.8 to 1.75, the crystal structure does not change in a qualitative way. As shown in Fig. 5, the measurements at all ξ agree well with hcp or rhcp structure. We take this as a strong argument for either hcp or rhcp structure with a tendency toward hcp. That the crystal structure does not change qualitatively in the studied ξ range is supported by the dependence of the peak positions determined from SANS and USANS measurements. The peaks at $q < 0.004$ Å^{-1} are found to shift according to $\xi^{1/3}$, as shown in Fig. 6, reflecting the isotropic shrinkage of the interparticle separation. At ξ=0.80 the position of the first peak corresponds to a nearest-neighbor distance of 460 nm, which is consistent with the size expected for a fully swollen microgel particle (Fig. 1).

The result from a typical SANS measurement of a crystalline sample is presented in Fig. 7. Due to the limited q resolution of the SANS instrument, the individual Bragg peaks cannot be resolved [31]. Perhaps the most remarkable feature of these measurements is the lack of well defined structural features. Only broad peaks containing an unknown

number of Bragg peaks are observed. As a result, these data do not allow us to confirm a crystal structure. The SANS and USANS results are consistent though: the fits for the different structures that are shown by the lines are obtained with the same structural parameters as the fits to the USANS measurements of Fig. 4. Furthermore, the positions of the first two broad peaks seen in SANS agree with those observed in USANS, as shown in Fig. 6.

IV. CONCLUSIONS

We find that even at very high densities, where particles must shrink, the crystal structure remains hcp or rhcp as at lower densities. Thus, the phase behavior does not differ fundamentally from that of hard spheres. This is in line with a rheology study of swollen microgel particles with screened charge repulsion, where also hard-sphere-like behavior was observed [11] and it might be due to the relatively high cross-linker concentration of 5 wt %, which could enhance steric repulsions between particles and render them stiffer, such that they crystallize in hard-sphere-like structures. For even softer microgels, with lower cross-linker concentration, the situation might change and noncubic crystal structures might form, as expected in Ref. [8].

ACKNOWLEDGMENTS

B.S.M. and A.F.N. thank Ministerio de Ciencia y Tecnología (DPI2008-06624-C03-03) for support and University of Almeria. U.G. was financially supported by the Adolphe Merkle Foundation. USANS measurements were performed at the National Institute of Standards and Technology (NIST), U.S. Department of Commerce, Gaithersburg, MD; we thank A. Jackson for his help during the measurements. SANS was performed at both NIST and at the Swiss spallation neutron source SINQ, Paul Scherrer Institute, Villigen, Switzerland.

[1] D. J. Beebe, J. S. Moore, J. M. Bauer, Q. Yu, R. H. Liu, C. Devadoss, and B.-H. Jo, Nature (London) **404**, 588 (2000).
[2] S. V. Vinogradov, T. K. Bronich, and A. V. Kabanov, Adv. Drug Delivery Rev. **54**, 135 (2002).
[3] M. J. Serpe, J. Kim, and L. A. Lyon, Adv. Mater. **16**, 184 (2004).
[4] B. R. Saunders and B. Vincent, Adv. Colloid Interface Sci. **80**, 1 (1999).
[5] V. Anderson and H. Lekkerkerker, Nature (London) **416**, 811 (2002).
[6] L. Cipelletti and L. Ramos, J. Phys.: Condens. Matter **17**, R253 (2005).
[7] R. P. Sear, J. Phys.: Condens. Matter **19**, 033101 (2007).
[8] D. Gottwald, C. N. Likos, G. Kahl, and H. Löwen, Phys. Rev. Lett. **92**, 068301 (2004).
[9] P. S. Mohanty and W. Richtering, J. Phys. Chem. B **112**, 14692 (2008).
[10] T. Hellweg, C. D. Dewhurst, E. Brueckner, K. Kratz, and W. Eimer, Colloid Polym. Sci. **278**, 972 (2000).
[11] J. J. Crassous, M. Siebenbürger, M. Ballauff, M. Drechsler, O. Henrich, and M. Fuchs, J. Chem. Phys. **125**, 204906 (2006).
[12] P. Ziherl and R. D. Kamien, Phys. Rev. Lett. **85**, 3528 (2000).
[13] A. Loxley and B. Vincent, Colloid Polym. Sci. **275**, 1108 (1997).
[14] A. Guillermo, J. P. C. Addad, J. P. Bazile, D. Duracher, A. Elaissari, and C. Pichot, J. Polym. Sci., Part B: Polym. Phys. **38**, 889 (2000).
[15] D. Duracher, A. Elaissari, and C. Pichot, J. Polym. Sci., Part A: Polym. Chem. **37**, 1823 (1999).
[16] A. Fernandez-Nieves, F. d. l. Nieves, and A. Fernandez-Barbero, J. Chem. Phys. **120**, 374 (2004).
[17] M. Stieger, W. Richtering, J. Pedersen, and P. Lindner, J. Chem. Phys. **120**, 6197 (2004).
[18] I. Berndt, J. S. Pedersen, and W. Richtering, J. Am. Chem. Soc. **127**, 9372 (2005).
[19] T. G. Mason and M. Y. Lin, Phys. Rev. E **71**, 040801 (2005).
[20] A. Fernandez-Barbero, A. Fernandez-Nieves, I. Grillo, and E. Lopez-Cabarcos, Phys. Rev. E **66**, 051803 (2002).
[21] A. Fernandez-Nieves, A. Fernandez-Barbero, B. Vincent, and F. d. l. Nieves, Macromolecules **33**, 2114 (2000).
[22] H. Senff and W. Richtering, J. Chem. Phys. **111**, 1705 (1999).
[23] J. Barker, C. Glinka, J. Moyer, M. Kim, A. Drews, and M. Agamalian, J. Appl. Crystallogr. **38**, 1004 (2005).
[24] M. R. Eskildsen, P. L. Gammel, E. D. Isaacs, C. Detlefs, K. Mortensen, and D. J. Bishop, Nature (London) **391**, 563 (1998).
[25] S. Hendricks and E. Teller, J. Chem. Phys. **10**, 147 (1942).
[26] P. N. Pusey, W. van Megen, P. Bartlett, B. J. Ackerson, J. G. Rarity, and S. M. Underwood, Phys. Rev. Lett. **63**, 2753 (1989).
[27] V. S. K. Balagurusamy, G. Ungar, V. Percec, and G. Johansson, J. Am. Chem. Soc. **119**, 1539 (1997).
[28] T. Cagin, G. Wang, R. Martin, G. Zamanakos, N. Vaidehi, D. T. Mainz, and W. A. Goddard III, Comput. Theor. Polym. Sci. **11**, 345 (2001).
[29] M. Hanfland, K. Syassen, N. E. Christensen, and D. L. Novikov, Nature (London) **408**, 174 (2000).
[30] J. Crain, S. J. Clark, G. J. Ackland, M. C. Payne, V. Milman, P. D. Hatton, and B. J. Reid, Phys. Rev. B **49**, 5329 (1994).
[31] C. Dewhurst, Meas. Sci. Technol. **19**, 1 (2008).